

# ON THE ORIGIN OF TEV GAMMA-RAY EMISSION FROM HESS J1834–087

R. MUKHERJEE<sup>1</sup>, E. V. GOTTHELF<sup>2</sup>, AND J. P. HALPERN<sup>2</sup>

(Received 26 June 2008; Accepted 3 October 2008)  
*The Astrophysical Journal*

## ABSTRACT

We present an X-ray study of the field containing the extended TeV source HESS J1834–087 using data obtained with the *XMM-Newton* telescope. Previously, the coincidence of this source with both the shell-type supernova remnant (SNR) W41 and a giant molecular cloud (GMC) was interpreted as favoring  $\pi^0$ -decay  $\gamma$ -rays from interaction of the old SNR with the GMC. Alternatively, the TeV emission has been attributed to inverse Compton scattering from leptons deposited by PSR J1833–0827, a pulsar assumed to have been born in W41 but now located 24' from the center of the SNR (and the TeV source). Instead, we argue for a third possibility, that the TeV emission is powered by a previously unknown pulsar wind nebula located near the center of W41. The candidate pulsar is XMMU J183435.3–084443, a hard X-ray point source that lacks an optical counterpart to  $R > 21$  and is coincident with diffuse X-ray emission. The X-rays from both the point source and diffuse feature are evidently non-thermal and highly absorbed. A best fit power-law model yields photon index  $\Gamma \sim 0.2$  and  $\Gamma \sim 1.9$ , for the point source and diffuse emission, respectively, and 2–10 keV flux  $\approx 5 \times 10^{-13}$  ergs cm<sup>-2</sup> s<sup>-1</sup> for each. At the measured 4 kpc distance of W41, the observed X-ray luminosity implies an energetic pulsar with  $\dot{E} \sim 10^{36}$  d<sub>4</sub><sup>2</sup> ergs s<sup>-1</sup>, which is also sufficient to generate the observed  $\gamma$ -ray luminosity of  $2.7 \times 10^{34}$  d<sub>4</sub><sup>2</sup> ergs s<sup>-1</sup> via inverse Compton scattering.

*Subject headings:* gamma-rays: individual (HESS J1834–087, G23.234–0.317) — gamma-rays: observations — pulsars: individual (PSR J1833–0827, XMMU J183435.3–084443)

## 1. INTRODUCTION

The HESS atmospheric Cherenkov telescope system has surveyed the Galactic plane with unprecedented sensitivity and spatial resolution, revealing  $\approx 50$  previously unknown sources of TeV ( $> 10^{11}$  eV)  $\gamma$ -ray emission (Aharonian et al. 2006a, 2008). About half of the Galactic TeV sources detected by HESS are identified with supernova products<sup>3</sup> – supernova remnants (SNRs) or pulsar wind nebulae (PWNe), which is a likely scenario for many of the unclassified sources as well. For PWNe, the leading explanation for the generation of TeV emission is leptonic, inverse Compton scattering of the microwave background or possibly ambient IR photons (Aharonian et al. 2006b). TeV  $\gamma$ -rays can also arise from the decay of neutral pions created in hadronic collisions of high-energy protons with the ambient medium.

The origin of HESS J1834–087 is a matter of great interest. This extended source (5.4' radius at 1  $\sigma$ ) lies close to the center of the large (27' diameter) shell-type SNR W41 (G23.3–0.3) and has a  $\gamma$ -ray flux of 8% that of the Crab above 200 GeV (Aharonian et al. 2006a). The TeV flux and extended nature of HESS J1834–087 were confirmed with the MAGIC  $\gamma$ -ray telescope (Albert et al. 2006). Based on VLA Galactic plane survey data, CO molecular line data, and an X-ray observation, Tian et al. (2007) argue that this TeV source could be  $\pi^0$ -decay  $\gamma$ -rays from the interaction of the old ( $\sim 10^5$  yr) SNR W41 with a giant molecular cloud (GMC), as envisioned by Yamazaki et al. (2006). This would be an

important result showing that old SNR shells are potential sources of cosmic rays. Alternatively the location of the pulsar PSR J1833–0827, 24' from the center of HESS J1834–087, prompted Bartko & Bednarek (2008) to favor it as a source of relativistic electrons, injected earlier at the birthplace of the pulsar, to power the TeV emission.

Herein, we present further X-ray analysis of the *XMM-Newton* observation of HESS J1834–087. We detect a point source and associated diffuse emission at the center of W41, which are likely a pulsar and wind nebula. This is a hard, non-thermal point source in the *XMM-Newton* image, and it lacks an optical/IR counterpart. Based on the morphological and spectral evidence, we argue that this point source is a pulsar that could power the observed TeV emission from HESS J1834–087, as in other PWNe.

## 2. DATA ANALYSIS AND RESULTS

The field containing HESS J1834–087 was observed by *XMM-Newton* for 20 ks on 2005 September (P.I. Pühlhofer, ObsID 0302560301). Tian et al. (2007) have already analyzed the data from the pn detector of the European Photon Imaging Camera (EPIC). Here, we complete the study of this observation by including data from the two EPIC MOS CCD cameras (MOS1 and MOS2). These instruments were operated in “full frame” mode using the medium filter with HESS J1834–087 located at the center of the 0.5° diameter field-of-view. This mode provides a time resolution of 2.6 s, insufficient to search for a signal from a typical rotation-powered pulsar. We analyzed standard data products obtained from the *XMM-Newton* archive (processed with the xmm-sas\_20050428.1800-6.0.0 pipeline) using both the SAS and FTOOLS software. The observation was contam-

<sup>1</sup> Department of Physics & Astronomy, Barnard College, Columbia University, New York, NY 10027

<sup>2</sup> Columbia Astrophysics Laboratory, Columbia University, New York, NY 10027

<sup>3</sup> [http://www.mpi-hd.mpg.de/hfm/HESS/public/HESS\\_catalog.htm](http://www.mpi-hd.mpg.de/hfm/HESS/public/HESS_catalog.htm)

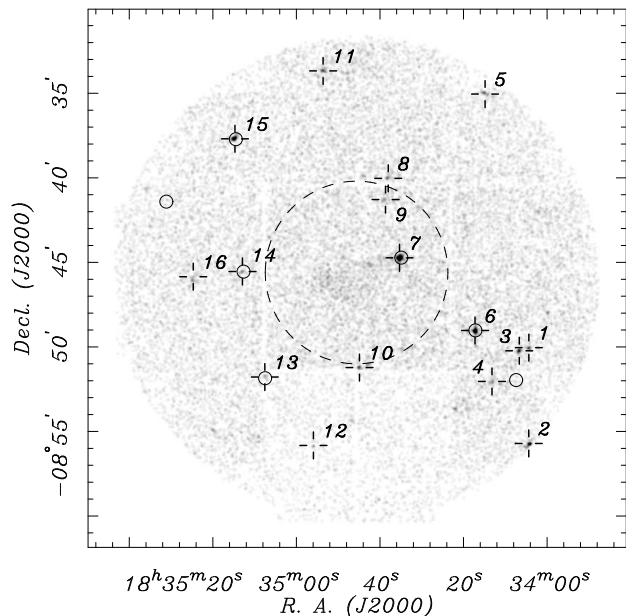


FIG. 1.— *XMM-Newton* MOS exposure corrected image of the HESS J1834–087 field in the 1.5–7 keV energy band, selected to best reveal the central diffuse emission. The dashed circle is the  $1\sigma$  extent of the TeV source. Significant *XMM-Newton* point sources are numbered; their properties are listed in Table 1. XMMU J183435.3–084443 (source 7), the hardest source in the *XMM-Newton* data, falls within the central  $\gamma$ -ray emission. The seven small circles mark the locations of sources detected in *Swift* XRT images.

inated by several intervals of high particle background, which were filtered out to leave a total of 13.86 ks of good observing time per detector. Details of the EPIC pn observation can be found in Tian et al. (2007).

We constructed exposure corrected, merged images from the two MOS cameras in various X-ray energy bands. Figure 1 shows the full *XMM-Newton* MOS 1.5–7 keV X-ray image of the HESS J1834–087 field with the significant ( $> 4\sigma$ ) point sources marked. The dashed circle indicates the  $1\sigma$  extent of the TeV emission (Aharonian et al. 2006a). Table 1 lists the basic X-ray data on the point sources, and the most likely USNO-B1.0 and/or 2MASS counterparts of some of them. XMMU J183435.3–084443 (source 7) is the hardest one. In the EPIC-pn detector, source 7 fell on a gap between the CCDs, so it appears as two faint point sources in the image analysis of Tian et al. (2007, Fig. 4). It is also detected by the *Swift* X-ray telescope (XRT) in an observation of the HESS J1834–087 field by Landi et al. (2006) (see §2.1).

Figure 2 is a zoom-in on the region near source 7, showing the diffuse X-ray emission, hereafter referred to as G23.234–0.317, extending from the point source throughout much of the central part of the TeV emission. Compared to the image analysis of the EPIC pn data by Tian et al. (2007), the extent of the diffuse X-ray emission is significantly larger and clearly merges with the hard point source. It lies near the center of the SNR, in a region of enhanced radio emission.

We extracted spectra for source 7 and G23.234–0.317 using data from each EPIC instrument and fitted them to a power-law model using the XSPEC software. For the

point source we used a radius  $r = 0.5'$  circular aperture and a concentric  $1' < r \leq 1.7'$  annular background region. The diffuse emission is extracted from a triangular region (see Fig. 2) with the point source region excluded; the background is a  $r = 4'$  circle with this diffuse region punched out. Spectra from the two MOS cameras were summed. Fitting of these spectra is limited by the small number of source counts for each region per EPIC instrument, which were grouped with a minimum of 40 or 20 counts per spectral channel for the pn and MOS point source data, respectively, and 150 counts per channel for the diffuse emission. The pn counts for the point source are 2/3 of the summed MOS counts because most of the pn counts are lost in the gap between the CCDs. Spectra from both regions are evidently highly absorbed as the flux below 2 keV is strongly cut off.

Figure 3 shows the pairs of spectra from each region and instrument fitted to an absorbed power law with column density  $N_H$  and photon index  $\Gamma$  tied for each extraction region. Although we cannot distinguish between continuum spectral models, we see no evidence of line emission in the background subtracted spectra. Table 2 presents the best-fit spectral parameters along with the measured flux, taken as the average of the EPIC MOS and pn. Although the error on each parameter is large, the estimated 2–10 keV fluxes are fairly robust for the range of allowed values. Although the X-ray measured column density for source 7 and G23.234–0.317 is not well constrained, it likely exceeds the integrated Galactic total<sup>4</sup> in this direction of  $N_H = 2 \times 10^{22} \text{ cm}^{-2}$ , suggesting that molecular material may lie in front of this structure. In Table 2 we also present spectral fits allowing independent values for the column density of each region.

### 2.1. *Swift* Observations

The TeV field of HESS J1834–087 was observed with the *Swift* X-ray telescope (XRT) in photon counting mode on three occasions, logged in Table 3. The first observation on 2005 June 29 UT is described by Landi et al. (2006). They identified three sources, of which two are detected by *XMM-Newton* at  $> 4\sigma$  significance. Two subsequent observation, obtained on 2007 March 11 and 2008 February 15 UT, reveal a total of seven sources detected at the  $> 3\sigma$  significance level (marked with circles in Fig. 1). We extracted background subtracted count rates for source 7 from each observation to search for variability. The counts derived from the third observation show a  $3\sigma$  increase over the first two, or  $2\sigma$  over the mean rate (see Table 3). This range of count rates is consistent with the *XMM-Newton* measured flux in Table 2. Using the PIMMS software, the *XMM-Newton* flux of source 7 predicts a 2–10 keV *Swift* count rate of  $(2-4) \times 10^{-3} \text{ s}^{-1}$ . Given the large uncertainty in both the *XMM-Newton* spectral fit and the *Swift* counts, we can make no firm conclusion about intrinsic flux variability of source 7, a possibility that cannot be excluded.

## 3. DISCUSSION

The spectral properties of source 7 distinguish it from the local field stars by its hard, non-thermal emission.

<sup>4</sup> Galactic  $N_H$  calculator available at [heasarc.gsfc.nasa.gov/cgi-bin/Tools/w3nh/w3nh.pl](http://heasarc.gsfc.nasa.gov/cgi-bin/Tools/w3nh/w3nh.pl)

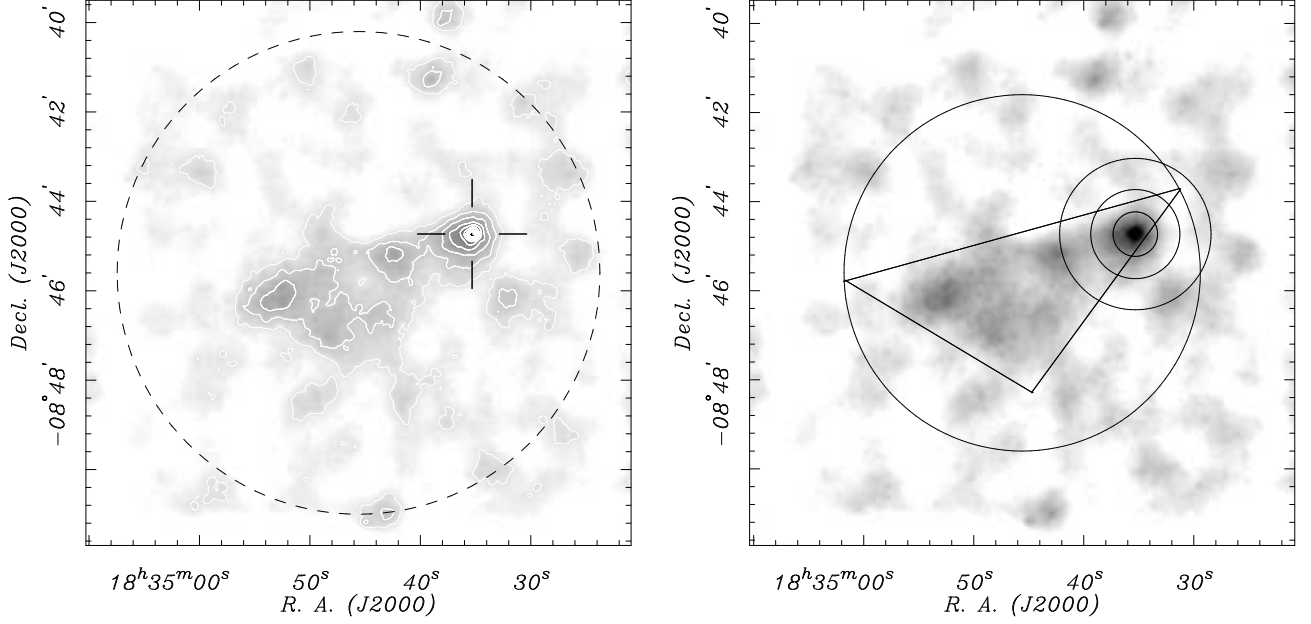


FIG. 2.— A zoom-in on the HESS J1834–087 region shown in Figure 1. *Left:* Image is smoothed and scaled to highlight the central diffuse emission and its connection to point source 7 marked by the cross. The greyscale intensity is linear and the contours are uniformly spaced. The dashed circle reproduces the  $1\sigma$  extent of the TeV source. *Right:* Outlines of the spectral extraction and background regions described in the text.

TABLE 1  
POINT SOURCES IN *XMM-Newton* OBSID 0302560301 AND NEAREST OPTICAL/IR CANDIDATES

No.	X-ray Position (J2000.0)		$N_s^a$ (cts)	$N_h^a$ (cts)	HR <sup>a</sup>	Opt./IR Position (J2000.0)		$B2^b$ (mag)	$R2^b$ (mag)	$J^c$ (mag)	$H^c$ (mag)	$K^c$ (mag)	Offset (")
	R.A.	Decl.				R.A.	Decl.						
1..	18 34 04.38	−08 50 02.7	121	15	−0.78	...	...	...	...	...	...	...	...
2..	18 34 04.38	−08 55 42.6	1	67	0.97	18 34 04.42	−08 55 42.4	20.89	18.93	16.04	15.17	13.47	0.6
3..	18 34 06.67	−08 50 13.8	18	110	0.71	18 34 06.67	−08 50 15.1	...	...	...	14.60	12.98	1.4
4..	18 34 13.20	−08 52 02.7	29	25	−0.08	...	...	...	...	...	...	...	...
5..	18 34 14.85	−08 35 02.8	96	56	−0.26	18 34 14.70	−08 35 01.1	17.13	14.87	12.27	11.59	11.37	2.9
6..	18 34 17.24	−08 49 01.8	66	140	0.36	18 34 17.28	−08 49 01.8	...	...	...	...	...	...
7..	18 34 35.32	−08 44 43.8	0	258	1.00	...	...	...	...	...	...	...	...
8..	18 34 38.02	−08 40 01.9	40	11	−0.58	...	...	...	...	...	...	...	...
9..	18 34 38.67	−08 41 17.3	38	55	0.19	18 34 38.75	−08 41 19.2	...	...	16.30	15.23	...	2.3
10..	18 34 44.90	−08 51 13.3	2	80	0.96	18 34 45.00	−08 51 10.3	19.98	16.39	...	...	...	0.9
11..	18 34 53.61	−08 33 40.6	30	18	−0.26	...	...	...	...	...	...	...	...
12..	18 34 55.93	−08 55 49.6	9	16	0.25	...	...	...	...	...	...	...	...
13..	18 35 07.57	−08 51 46.9	44	51	0.07	...	...	...	...	...	...	...	...
14..	18 35 12.91	−08 45 34.6	0	57	1.00	...	...	...	...	...	...	...	...
15..	18 35 14.71	−08 37 41.5	158	147	−0.04	18 35 14.66	−08 37 40.6	...	...	14.71	11.76	10.42	1.3
16..	18 35 24.70	−08 45 51.0	35	59	0.26	...	...	...	...	...	...	...	...

NOTE. — Units of right ascension are hours, minutes, and seconds, and units of declination are degrees, arcminutes, and arcseconds.

<sup>a</sup>Background subtracted counts using data from all EPIC detectors. Hardness ratio defined as  $HR = (N_h - N_s) / (N_h + N_s)$ , where  $N_s$  and  $N_h$  are the counts in the 0.3–2 keV and 2–10 keV bands, respectively.

<sup>b</sup>Magnitude from the USNO-B1.0 Catalog.

<sup>c</sup>Magnitude from the 2MASS Catalog.

Coupled with the lack of an optical/IR counterpart, this favors a compact object. Its spectrum is flatter than that of the typical AGN. It is also notable that source 7 lies at a plausible birth place for a pulsar, the center of the shell-type SNR W41, and is located  $3'$  from the centroid of HESS J1834–087, well within its  $10'$  diameter ( $1\sigma$ ) extent. Finally, its location at one of the vertexes of the patch of diffuse X-ray emission uniquely suggests that source 7 is a pulsar generating a PWN, G23.234–0.317, and also HESS J1834–087. However, possible flux variability among *Swift* pointings, if significant, would prefer

an X-ray binary, unlikely to be associated with the extended TeV source. Pending further evidence of variability, a pulsar scenario remains the preferred hypotheses for the TeV emission.

In PWNe, relativistic  $e^\pm$  are accelerated by the pulsar and its wind termination shock, and TeV photons may be produced by inverse Compton scattering of the cosmic microwave background, interstellar and stellar IR/optical photons, or low-energy synchrotron photons. If the accelerated particles include protons, which collide with the ambient medium making pions, TeV  $\gamma$ -rays may

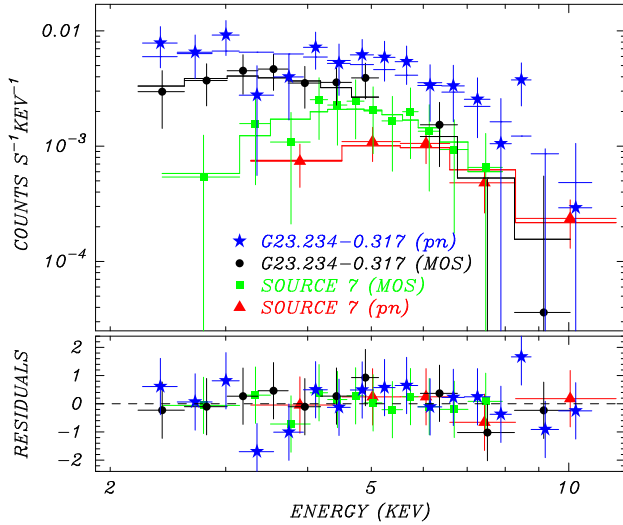


FIG. 3.— *XMM-Newton* spectra of source 7 in the MOS (squares) and pn (triangles), and the diffuse source G23.234–0.317 (MOS: circles, pn: stars) fitted to the power-law model described in the text. Residuals from this fit are displayed in the lower panel.

TABLE 2  
*XMM-Newton* SPECTROSCOPY

Parameter	Source 7	G23.234–0.317
$N_H$ (cm $^{-2}$ )	$6.0^{+2.6}_{-5.3} \times 10^{22}$	tied
$\Gamma$	$0.2^{+0.9}_{-1.0}$	$1.9^{+1.0}_{-0.9}$
$F_x$ (ergs s $^{-1}$ cm $^{-2}$ ) <sup>a</sup>	$4.9 \times 10^{-13}$	$4.0 \times 10^{-13}$
$\chi^2$ (dof)	0.64(20)	
$N_H$ (cm $^{-2}$ )	$13^{+31}_{-12} \times 10^{22}$	$3.3^{+5.5}_{-1.8} \times 10^{22}$
$\Gamma$	$0.88^{+1.9}_{-0.85}$	$1.5^{+1.2}_{-1.0}$
$F_x$ (ergs s $^{-1}$ cm $^{-2}$ ) <sup>a</sup>	$4.8 \times 10^{-13}$	$4.2 \times 10^{-13}$
$\chi^2$ (dof)	0.63(21)	

<sup>a</sup>Absorbed flux averaged for the two EPIC instruments in the 2–10 keV energy band.

also be the product of  $\pi^0$  decay. For HESS J1834–087, target material is readily available in the GMC in the vicinity of the SNR W41 or in the supernova shell itself. The *Midcourse Space Experiment* 21 $\mu$ m survey data reveals cold dust in the two lobes of the molecular cloud found in CO by Tian et al. (2007); however, these do not align well with the diffuse X-ray emission. Finally, there are several bright HII regions within 10' of the TeV source that are potential sources of seed photons.

### 3.1. PWN X-ray and $\gamma$ -ray Energetics

Energetically, if XMMU J183435.3–084443 is associated with W41 at a distance of 4 kpc (Tian et al. 2007), its 2–10 keV luminosity is  $L_x = 9 \times 10^{32} d_4^2$  ergs s $^{-1}$ . This implies a spin-down luminosity from a rotation-powered pulsar of  $\dot{E} \sim 10^{36}$  erg s $^{-1}$  (Possenti et al. 2002), near the empirical threshold of  $\dot{E}_c > 4 \times 10^{36}$  ergs s $^{-1}$  for generating a bright ( $F_{PWN}/F_{PSR} \gtrsim 1$ ; 2–10 keV) PWN (Gotthelf 2004). Our measured flux ratio of  $F_{PWN}/F_{PSR} \approx 1$  is at the low end for pulsars above  $\dot{E}_c$ , but is similar to some other *HESS* sources associated with PWNe. Most notably, the 2–10 keV flux ratio for the energetic ( $\dot{E} = 5.5 \times 10^{36}$  ergs s $^{-1}$ ) pulsar PSR J1838–0655 as-

TABLE 3  
*Swift* XRT DETECTIONS OF *XMM-Newton* SOURCE 7

Parameter	2005 Jun 29 (UT)	2007 Mar 11 (UT)	2008 Feb 15 (UT)
ObsID	00035159001	00035159002	00035117003
Exposure (s)	5977	5019	6183
Counts <sup>a</sup>	$12 \pm 4.0$	$9.8 \pm 3.6$	$32 \pm 6.0$
Rate (10 $^{-3}$ s $^{-1}$ ) <sup>a</sup>	$2.0 \pm 0.7$	$1.9 \pm 0.7$	$5.1 \pm 1.0$

<sup>a</sup>Background subtracted counts and count rate in a 1/4 diameter aperture in the 2–10 keV energy band.

sociated with HESS J1837–069 is  $F_{PWN}/F_{PSR} \sim 0.1$  (Gotthelf & Halpern 2008).

HESS J1834–087 is detected up to 3 TeV. However, if we extrapolate and integrate its  $\Gamma = 2.45$  power-law (Aharonian et al. 2006a) from 0.3 to 30 TeV for comparison with Gallant et al. (2008), we get an energy flux of  $1.4 \times 10^{-11}$  ergs cm $^{-2}$  s $^{-1}$ , corresponding to a luminosity of  $L_\gamma = 2.7 \times 10^{34} d_4^2$  ergs s $^{-1}$  at the location of W41 (Albert et al. 2006). Under the assumption that the putative pulsar XMMU J183435.3–084443 powers the observed TeV emission, the estimated efficiency (0.3 – 30 TeV) is  $\epsilon \equiv L_\gamma/\dot{E} \sim 3\%$ . This is consistent with the range of efficiencies (0.01 – 11%) found for other very-high-energy PWNe candidates (Gallant et al. 2008). Compared to the X-ray luminosity, the  $\gamma$ -ray emission clearly dominates, with a ratio of  $L_\gamma/L_x \approx 29$ . This is similar to the value  $L_\gamma/L_x \approx 33$  found for the apparent PWN association of G338.3–0.0 with HESS J1640–465 (Funk et al. 2007). Several authors have hypothesized that such high flux ratios are possible from inverse Compton scattering when PWNe are bathed in infrared seed photons from nearby H II regions, e.g., W33 close to HESS J1813–178 (Helfand et al. 2007), or the massive star cluster RSGC1 near HESS J1837–069 (Gotthelf & Halpern 2008). A similar scenario may apply to the bright TeV PWNe that are displaced from their pulsar power sources, e.g., HESS J1825–137/PSR B1823–13 (Pavlov et al. 2008).

### 3.2. Alternative Hypotheses

One of the surprises of the TeV era is the offset of many HESS sources from the PWNe nominally responsible for powering the  $\gamma$ -ray emission. With this displacement in mind, some authors consider the 85 ms pulsar PSR J1833–0827 that lies 24' north of W41 as a potential source of accelerated particles powering HESS J1834–087. A possible association of PSR J1833–0827 with W41 was mentioned by Clifton & Lyne (1986) and was deemed plausible by Gaensler & Johnston (1995). Weisberg et al. (1995) derived a kinematic distance of 4–5 kpc for PSR J1833–0827 from H I absorption, which is compatible with the H I distance of  $4.1 \pm 0.3$  kpc to W41 (Leahy & Tian 2008). Tian et al. (2007) also noted that the  $1.5 \times 10^5$  yr characteristic age of PSR J1833–0827 is consistent with the  $\approx 10^5$  yr age that they estimated for W41. Furthermore, a large proper motion of  $33 \pm 5$  mas yr $^{-1}$  toward positive Galactic latitude, a direction away from W41, was measured for PSR J1833–0827 by Hobbs et al. (2005). At  $d = 4.1$  kpc, this corresponds to a not implausible tangential velocity  $v_t = 640$  km s $^{-1}$ . In  $1 \times 10^5$  yr, PSR J1833–0827

would have traveled  $55'$ , even further than its present offset from W41. Although the spin-down luminosity ( $\dot{E} = 5.8 \times 10^{35}$  ergs s $^{-1}$ ) of this pulsar could be sufficient to power HESS J1834–087, Aharonian et al. (2006a) felt that the large separation renders an association unlikely.

Without regard to its known proper motion, Bartko & Bednarek (2008) advocate PSR J1833–0827 as the source of HESS J1834–087, assuming that the pulsar has  $v_t \sim 250$  km s $^{-1}$ . They hypothesized that prior injection of leptons by the pulsar while near its birth location powers the currently observed TeV emission by inverse Compton scattering. However, given our detection of a putative pulsar/PWN inside W41 and coincident with HESS J1834–087, we consider that our candidate is more likely the source of HESS J1834–087, probably with a spin-down luminosity  $\dot{E} > 10^{36}$  ergs s $^{-1}$ , and that the nearby PSR J1833–0827 is a chance coincidence, possibly a product of the frequent birth of pulsars in active star formation regions.

The location of GMCs near SNR W41 led Tian et al. (2007) to explore the possibility that the TeV emission from HESS J1834–087 might result from the interaction between the two. Yamazaki et al. (2006) considered the production of TeV gamma rays in older SNR shells and from the SNR shock running into a GMC, using the diagnostic ratio of TeV to X-ray flux to distinguish between the different possibilities. They suggest that this ratio is of order 10 to 100 for TeV gamma-ray emission from the SNR, but lower ( $\sim 10$ ) for a SNR shock running into a GMC. The flux ratio  $F_\gamma(1 - 10 \text{ TeV})/F_x(2 - 10 \text{ keV})$  obtained by Tian et al. (2007) and this work is consistent

with both of these scenarios. TeV gamma-ray production due to the interaction of high energy protons from the SNR shock with the GMC is, however, unlikely; based on Yamazaki et al. (2006), this would require a much higher TeV/X-ray flux ratio of  $> 100$ .

#### 4. CONCLUSIONS

The Galactic TeV sources detected by HESS include, by our count,  $\approx 20$  PWN counterparts (see also Gallant et al. 2008; Hessels et al. 2008) and a few more possible PWN associations, making this the largest class of identified Galactic high energy sources. While it is plausible that HESS J1834–087 is associated with the GMC located at the center of W41 as argued by Tian et al. (2007), we believe that our detection of a putative pulsar/PWN candidate XMMU J183435.3–084443/G23.234–0.317 within the extent of HESS J1834–087 suggests a more likely scenario. The X-ray and  $\gamma$ -ray morphology and flux ratio are consistent with the TeV source being powered by a pulsar/PWN. Deeper X-ray timing observations can be performed to search for pulsations from XMMU J183435.3–084443, which will be invaluable to test this scenario and determine more quantitatively the energetics of this system.

RM was supported in part by the National Science Foundation under grant no. PHY-0601112. EVG acknowledges *Chandra* grant SAO AR7-8004X.

#### REFERENCES

- Aharonian, F., et al. 2006a, ApJ, 636, 777  
 ———. 2006b, A&A, 456, 245  
 ———. 2008, A&A, 477, 353  
 Albert, J., et al. 2006, ApJ, 643, L53  
 Bartko, H., & Bednarek, W. 2008, MNRAS, 385, 1105  
 Clifton, T. R., & Lyne, A. G. 1986, Nature, 320, 43  
 Funk, S., Hinton, J. A., Pühlhofer, G., Aharonian, F. A., Hofman, W., Reimer, O., & Wagner, S. 2007, ApJ, 662, 517  
 Gaensler, B. M., & Johnston, S. 1995, MNRAS, 275, L73  
 Gallant, Y. A., et al. 2008, AIP Conference Ser. 983, 40 Years of Pulsars: Millisecond Pulsars, Magnetars, and More, ed. C. Bassa, Z. Wang, A. Cumming, & V. M. Kaspi (Melville, NY: AIP), 195  
 Gotthelf, E. V., & Halpern, J. P. 2008, ApJ, 681, 515  
 Gotthelf, E. V. 2004, in Young Neutron Stars and their Environments, IAU Symp. 218, ed. F. Camilo & B. M. Gaensler (San Francisco: ASP), 225  
 Helfand, D. J., Gotthelf, E. V., Camilo, F., Semler, D. R., Becker, R. H., & White, R. L. 2007, ApJ, 665, 1297  
 Hessels, J. T. W., et al. 2008, ApJ, submitted (arXiv:0806.1200)  
 Hobbs, G., Lorimer, D. R., Lyne, A. G., & Kramer, M. 2005, MNRAS, 360, 974  
 Landi, R., Bassani, L., Malizia, A., Masetti, N., Stephen, J. B., Bazzano, A., Ubertini, P., Bird, A. J., & Dean, A. J. 2006, ApJ, 651, 190  
 Leahy, D. A., & Tian, W. W. 2008, AJ, 135, 167  
 Pavlov, G. G., Kargaltsev, O., & Briskin, W. F. 2008, ApJ, 675, 683  
 Possenti, A., Cerutti, R., Colpi, M., Merghetti, S. 2002, A&A, 387, 993  
 Tian, W. W., Li, Z., Leahy, D. A., & Wang, Q. D. 2007, ApJ, 657, L25  
 Weisberg, J. M., Siegel, M. H., Frail, D. A., & Johnston, S. 1995, ApJ, 447, 204  
 Yamazaki, R., Kazunori, K., Bamba, A., Yoshida, T., Tsuribe, T., & Takahara, F. 2006, MNRAS, 371, 1975